Title

Investigation of NH3 Emissions from New Technology Vehicles as a Function of Vehicle Operating Conditions

Permalink

https://escholarship.org/uc/item/0r02f536

Authors

Huai, Tao
Durbin, Thomas D.
Miller, J. Wayne
et al.

Publication Date

2003-10-03

Peer reviewed

Investigation of NH₃ Emissions from New Technology Vehicles as a Function of Vehicle Operating Conditions

TAO HUAI, THOMAS D. DURBIN,*
J. WAYNE MILLER, JOHN T. PISANO,
CLAUDIA G. SAUER, SAM H. RHEE, AND
JOSEPH M. NORBECK

Bourns College of Engineering, Center for Environmental Research and Technology (CE-CERT), University of California, Riverside, California 92521

The objective of this study was to measure ammonia (NH₃) emissions from modern technology vehicles since information is scarce about this important source of particulate matter (PM) precursors. Test variables included the emission level to which the vehicle was certified, the vehicle operating conditions, and catalyst age. Eight vehicles with low-emission vehicle (LEV) to super-ultralow-emission vehicle (SULEV) certification levels were tested over the Federal Test Procedure (FTP75), a US06 cycle, a hot running 505, a New York City Cycle (NYCC), and a specially designed Modal Emissions Cycle (MEC01v7) using both as-received and bench-aged catalysts. NH₃ emissions in the raw exhaust were measured by tunable diode laser (TDL) absorption spectroscopy. The results show that NH₃ emissions depend on driving mode and are primarily generated during acceleration events. More specifically, high NH₃ emissions were found for high vehicle specific power (VSP) events and rich operating conditions. For some vehicles, NH₃ emissions formed immediately after catalyst light-off during a cold start.

1. Introduction

Understanding the relationship between emissions and mode of vehicle operation is complex but also one of the most critical aspects of accurately quantifying vehicle emissions. In recent years, there has been an increased effort to develop more extensive databases of real-time vehicle emissions and subsequently utilize these data for model development. Using real-time data, Jimenez-Palacios et al. showed that emissions were a function of vehicle specific power (VSP) (*1*). The United States Environmental Protection Agency (EPA) is also developing a new Multi-Scale Motor Vehicle and Equipment Emissions System (MOVES) model that will utilize real-time data for emissions estimates (*2*). In a preliminary modeling "shootout," EPA concluded that approaches using both binning of data by operational mode as well as VSP were promising for modeling emissions (*2, 3*).

While there have been considerable efforts to characterize and understand real-time emissions of regulated pollutants, fewer data are available for emissions of unregulated mobile-source emissions such as ammonia (NH₃). NH₃ contributes to the production of secondary particulate matter (PM) as

ammonium nitrate (NH₄NO₃) and ammonium sulfate ((NH₄)₂-SO₄), and some recent studies have indicated that NH₃ emission rates from automobiles may be higher than previously estimated, although a wide range of NH₃ emissions estimates (from <0.002 to 0.140 g/km) have been reported for vehicles (*4–14*). At present, it is estimated that mobile sources in the greater Los Angeles area are the third largest source of NH₃ emissions and account for approximately 18% of the inventory (*15*).

Studies of the emission rates and the mechanisms of NH₃ formation in vehicle exhaust date back to the 1970s (*16–22*). Early studies showed that NH₃ formation can be attributed primarily to reactions that occur over the catalyst (*23–28*). The detailed reaction chemistry on the catalyst surface is complex and involves a number of different individual reactions (*29*). Gandhi and Shelef (*26, 27*) suggested that hydrogen produced in the water-gas shift reaction (CO + H₂O ↔ CO₂ + H₂) could be a major contributor to NH₃ formation through the overall reaction of 2NO + 2CO + 3H₂ → 2NH₃ + 2CO₂ or 2NO + 5H₂ → 2NH₃ + 2H₂O. Studies have also shown that the operating condition of the vehicle plays an important role in the formation of NH₃ in vehicle exhaust. Researchers have found that NH₃ emissions can be more prevalent under conditions where the vehicles are malfunctioning or running rich (*13, 21*) or over aggressive driving cycles (*7*). Remote sensing studies, on the other hand, have shown high NH₃ emission levels can also be found even under near stoichiometric conditions (*6*). Clearly, to better understand and eventually to model NH₃ emissions in vehicle exhaust, it is important to understand which factors contribute to NH₃ production, including vehicle technology and operating mode, catalyst technology and age, and the air/fuel ratio.

The objective of this study was to examine NH₃ emissions as a function of different vehicle operating conditions and to better understand the formation of NH₃ emissions in vehicle exhaust. For this study, eight vehicles with low-emission vehicle (LEV) to super-ultralow-emission vehicle (SULEV) certification were tested over the Federal Test Procedure (FTP75), a US06 cycle, a hot running 505, a New York City Cycle (NYCC), and a specially designed Modal Emissions Cycle (MEC01v7) (*30*). An important aspect of this study was the measurement of NH₃ emissions using a tunable diode laser (TDL). This instrument allows in-situ measurements of highly time-resolved NH₃ emissions in the raw exhaust. This paper discusses the results of this study and provides some preliminary insights that might be useful in better understanding NH₃ emissions from vehicles.

2. Experimental Procedures

2.1. Test Vehicles and Fuels. A total of eight 2000–2001 vehicles with 6,000–30,000 miles were tested as part of the study. A description of the test vehicles is provided in the Supporting Information. The test matrix was composed of late model vehicles and included two SULEV vehicles, two ultralow-emission vehicles (ULEV), and four LEV vehicles, as defined by California regulations.

The test fuel used for this project was a commercial California Phase 2 gasoline doped to 30 ppmw sulfur, a value close to the average sulfur level of California gasoline. The properties of the test fuel are provided in the Supporting Information.

2.2. Catalyst and Oxygen Sensor Aging. For this program, each vehicle was tested using its original equipment (OE) as-received catalyst and a bench-aged catalyst. Catalysts were

* Corresponding author phone: (909) 781-5794; fax: (909) 781-5790; e-mail: durbin@cert.ucr.edu.
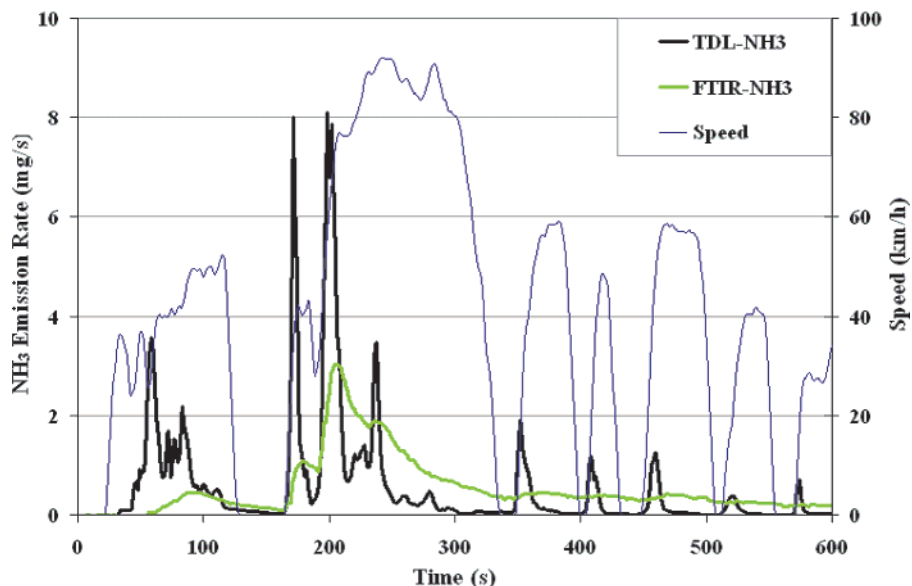
FIGURE 1. TDL vs FTIR NH$_3$ comparison.

aged for 90 h (120,000 mile equivalent) using the Rapid Aging Test-A (RAT-A) protocol at the Southwest Research Institute (SwRI) in San Antonio, TX (*31*). Catalysts were aged in pairs using a single V8 engine with the RAT-A temperature profile maintained for each catalyst and using a specially prepared ultralow 0.2 ppmw sulfur gasoline and a zero-sulfur oil (*32*).

2.3. Vehicle Testing Procedures. All vehicles were tested over a range of cycles including the FTP75, US06, MEC01v7, NYCC, and hot running 505. For all tests, standard bag and second-by-second measurements were obtained for total hydrocarbons (THC), non-methane hydrocarbons (NMHC), oxides of nitrogen (NO$_x$), and carbon monoxide (CO). NH$_3$ emission measurements are discussed below. Replicate tests were conducted over the FTP75 and US06 on each vehicle/ catalyst combination, with a third test conducted on a vehicle/ catalyst combination when the duplicates differed by more than the following criteria: THC 33%, NO$_x$ 29%, and CO 70% (*32*). For the other test cycles, only one test was conducted on both the aged and as-received catalyst for each vehicle.

The low-speed cycles included the FTP75, hot running 505, and NYCC. The FTP75 is a three-phase cycle designed to represent emissions under cold-start conditions (bag 1), hot stabilized operating conditions (bag 2), and hot-start conditions (bag 3). The hot running 505 is the same driving pattern as bags 1 and 3 of the FTP75, but the cycle is run with the vehicle fully warm. The NYCC test is designed to represent stop-and-go driving conditions in more congested city traffic. The high-speed cycles included the US06 and MEC01v7. The US06 is a cycle composed of aggressive, high-speed, and/or high-acceleration driving behavior, rapid speed fluctuations, and driving behavior that is not included in the FTP. The MEC01v7 is a cycle designed for the development of models to predict vehicle emissions from vehicle operating parameters (*30*).

2.4. NH$_3$ Measurements with a Tunable Diode Laser. Measurement of real-time NH$_3$ emissions from vehicles at the level required for comparison with other real-time parameters is difficult and required the implementation of a tunable diode near-infrared absorption spectrometer (TDL). Previous studies of real-time vehicle NH$_3$ emissions have more traditionally used Fourier transform infrared (FTIR) systems sampling through a dilution tunnel. The disadvantage of the FTIR system in a dilution is that there is considerable adsorption/desorption of NH$_3$ as the sample travels through the dilution tunnel as well as a sample

residence time in the FTIR of approximately 10 s. As a result, the FTIR measurements are broader, have an extended tail, and underestimate the peak NH$_3$ emissions. The TDL, on the other hand, provided the improved sensitivity and response time necessary to investigate low-level concentrations of exhaust NH$_3$ in real-time. A comparison of the two techniques is provided in Figure 1.

The advantages of the TDL were gained, in part, by making the measurements in-situ using raw exhaust gases rather than after significant dilution. The TDL was used in an extractive sampling system installed in conjunction with existing exhaust sampling lines for measuring raw pre- and postcatalyst emissions. The sampling cell was 2 m in length with a volume of approximately 1 L, and a corresponding residence time for the sample gas in the cell of just over 2 s. The cell was equipped with a retroreflector to double the effective optical path length of the 2-m section to 4 m. With the 4-m path length, the signal-to-noise ratio at two times the standard deviation was found to be better than 0.5 ppmv for a 2-s averaging time. The sampling system was heated at temperatures between 120 °C and 130 °C to prevent condensation and inhibit NH$_3$ adsorption in the sampling lines.

The diode laser controller used was a commercially available instrument, a LasIR, provided by Unisearch Associates Inc. The laser used was an InGaAsP, multiple quantum well (MQW), distributed feedback (DFB), type that had a central emission wavelength at 1.512 μm, with a tunability range greater than $\pm$20 nm. This wavelength corresponds to an overtone band of the N–H stretch vibration in the near-infrared spectral region. This laser type was chosen because it is virtually single mode with a side mode suppression ratio of better than 40 dB. The laser output was 5 mW, and it has a very fast response time on the order of 0.2 ns. The laser also has a very narrow bandwidth, 2.488 Gb/s, which is far narrower than the 1.5123 μm NH$_3$ absorption line which has a full width at half-maximum (fwhm) of 0.03 cm.

The absorption spectra were obtained by scanning the absorption feature every 1/64th of a second. Multiscan averaging was used to improve the sensitivity of the system. The spectra immediately before the absorption feature was included in this scan so that deviations in overall laser intensity could be measured, providing enhanced sensitivity. Two-tone FM modulation techniques were used to filter out any stray signals and to improve the signal-to-noise resolu-
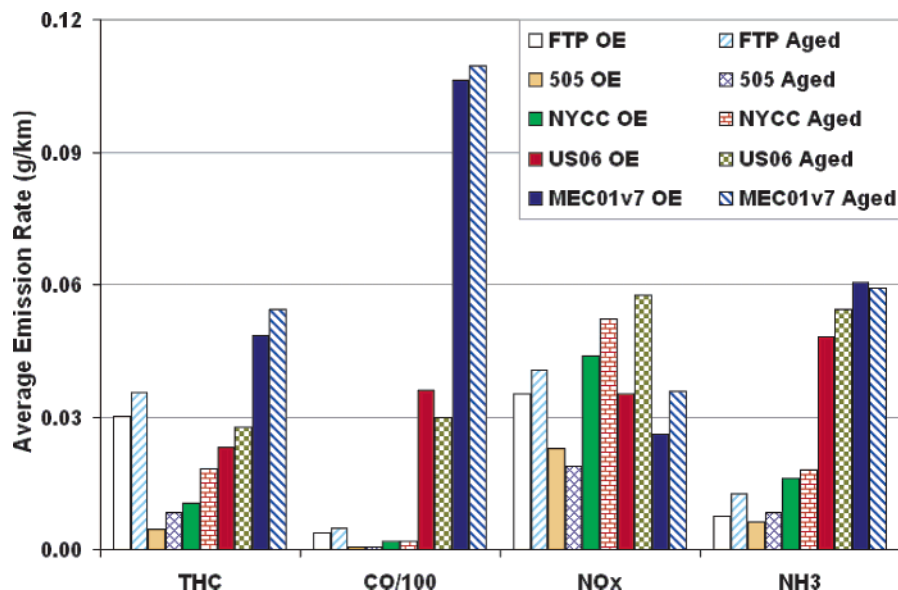
FIGURE 2. Average emissions vs cycles.

tion. This technique has been shown to approximate second derivative analysis, enhancing detection limits by at least a factor of 20 (*33*).

The dual channel capability of the TDL allowed the measurement of engine-out and tailpipe emissions simultaneously. The TDL was configured to provide data once every 2 s for both the engine-out and tailpipe emissions. For each channel, data were integrated over a 2-s dwell time, with sampling alternating between engine-out and tailpipe measurements each second. Second-by-second NH_3 concentrations were obtained using a linear interpolation. A slight offset was also observed in the background spectra due to a nearby water line which was accounted for in the background subtraction. The concentrations were then converted into mass emissions rates by multiplying by the density of NH_3 and the time-aligned exhaust flow rate (*30*). The exhaust flow rate was determined on a second-by-second basis using the CO_2 tracer method. Temperature and pressure corrections were applied to the TDL data based on second-by-second measurements made in the sampling cell.

Verification of the TDL accuracy was done using calibration gas levels between 10 and 150 ppmv. The calibration gas used for most of the verification tests and daily testing calibrations was certified with an accuracy of ±10%, typical of suggested accuracy levels for NH_3 calibration standards. The TDL readings were compared with measurements obtained from citric acid-coated filters at various positions in the sampling train. The results showed agreement within 10% for an NH_3 calibration gas level of 150 ppm.

The TDL also showed good agreement with a secondary FTIR technique that was used. In general, the TDL and FTIR NH_3 emissions were within ±10% for measurements made on the same test. Although the overall comparisons between the FTIR and TDL were relatively good, the limitations of the FTIR were observed for low NH_3 emission rates. In particular, for low NH_3 emission rates (i.e., below 6 mg/km) the FTIR typically underestimated NH_3 emissions since the peak NH_3 emissions could not be measured accurately and the emission levels in the tail region fell below the detection limits. For the US06 FTIR measurements, an additional problem occurred with the FTIR in that the tail for aggressive driving segments near the end of the test could not be fully quantified prior to the conclusion of the test.

3. Emissions Test Results

3.1. NH_3 Emissions for Different Driving Cycles.
Fleet average NH_3 emissions are presented in Figure 2 for each of

the five cycles for tests conducted on both as-received and aged catalysts. For comparison, fleet average THC, CO, and NO_x are also provided in Figure 2. The individual vehicle results for NH_3 are presented in Figure 3 for each of the test cycle/catalyst combinations. The results in Figure 3 are missing some data that were not obtained for vehicles SU1 and L2 for the as-received catalyst. The detailed test results are provided in the Supporting Information.

The data in Figures 2 and 3 show that NH_3 emissions vary from near zero to 0.144 g/km over all vehicles and cycles in this study. Over the low-speed cycles, such as the FTP, hot running 505, and NYCC, lower NH_3 emissions (typically below 0.020 g/km) were generally observed. The values can be compared with EPA NH_3 estimates for light-duty gasoline vehicles which average 0.063 g/km with a range from 0.001 g/km to 0.321 g/km (*16*). It should be noted that the EPA estimates are based on earlier studies and are more representative of older technology vehicles.

NH_3 emissions for the hot running 505 were comparable to those of the FTP, as expected since the 505 is driven over the same driving trace as those of bag 1 and bag 3 of the FTP. The FTP emissions were slightly higher than those for the 505, which can probably be attributed to different start conditions, as discussed below. The finding of slightly higher NH_3 emissions over the FTP compared with the hot running 505 was statistically significant at greater than a 95% confidence level for a paired *t*-test.

The NYCC is a low-speed cycle, but the driving conditions are more energy-intensive on a per-km basis than the FTP or 505, as shown in the Supporting Information by the higher CO_2 emission rates. On a fleet average basis, NH_3 emissions over the NYCC were slightly higher than those over the hot running 505 but were not statistically different from those for the FTP. For some vehicles with relatively low NH_3 emissions for the FTP cycle, the NH_3 emissions over the NYCC were considerably higher. For other vehicles, higher NH_3 emissions were found in the cold-start period leading to higher FTP NH_3 emissions.

NH_3 emissions increased considerably over the more aggressive US06 and MEC01v7 cycles. These cycles had the highest NH_3 emissions for nearly all of the vehicles, including vehicles that had relatively low NH_3 emissions over the FTP, hot running 505, or NYCC. This finding is consistent with previous studies that have shown that higher NH_3 emissions for higher loads or rich operating conditions (*13, 21*). One SULEV vehicle (SU1) showed almost no NH_3 emissions over
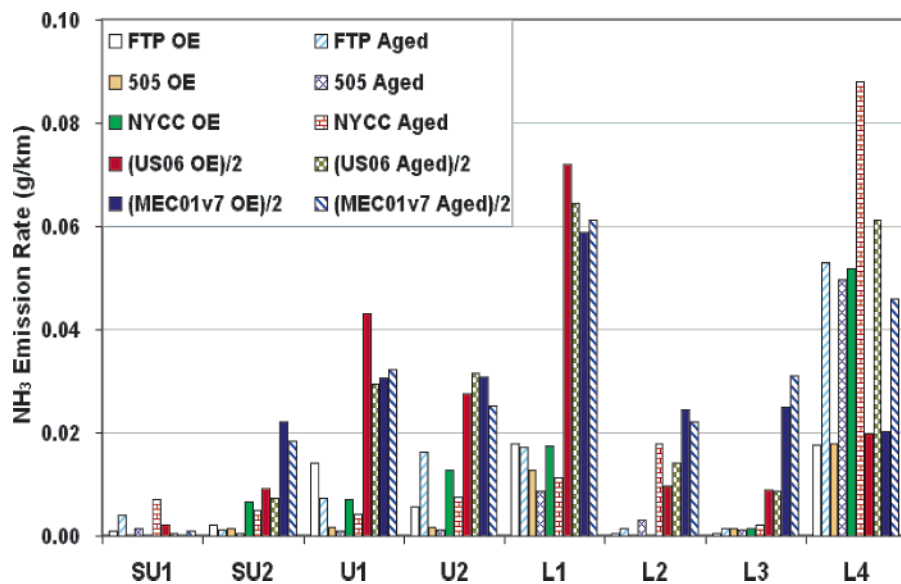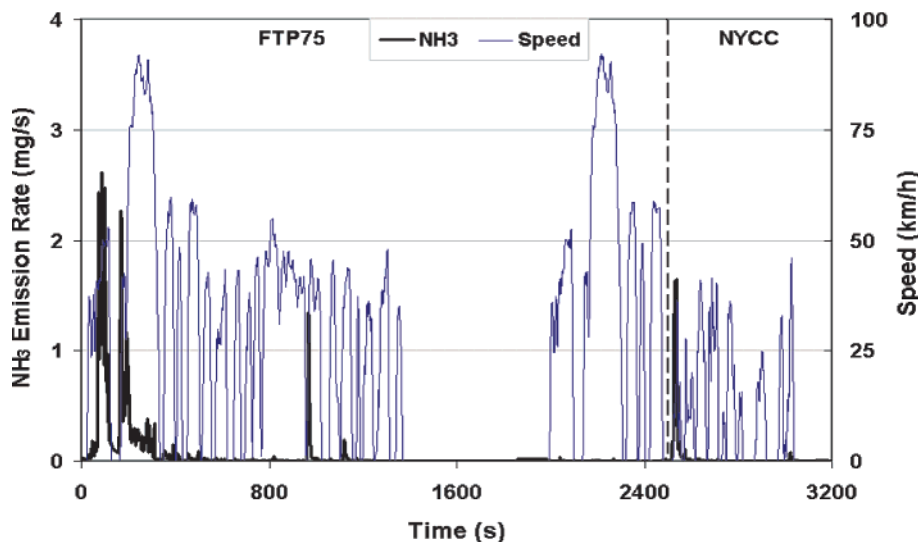
FIGURE 3. NH₃ emissions vs cycles.

FIGURE 4. Second-by-second NH₃ emissions for the FTP/NYCC (vehicle U2, OE Cat.).

either the US06 or MEC01v7 cycles, which may be attributable to the feedback and control technology used on this vehicle to maintain precise air/fuel (A/F) ratio (*34*). As discussed earlier, the MEC01v7 is primarily designed to facilitate the development of modal emissions models; hence, results over this cycle cannot be construed as being representative of real-world emissions, except under more aggressive conditions.

In general, NH_3 emission factors over the FTP were typically lower than those of the other regulated emissions, including THC, CO, and NO_x. For the FTP, it is important to note that a large fraction of the total cycle emissions for the regulated emissions are formed during the cold-start portion of the test or before catalyst light-off. For the hot running 505 and the NYCC, the catalyst is at full operating temperature, and fleet average NH_3 emissions were more comparable to THC emissions but still below those of NO_x and CO. For the more aggressive US06 and MEC01v7 cycles, fleet average NH_3 emissions were actually slightly higher than those of THC and NO_x. Interestingly, the trend in NH_3 emissions was similar to that observed for CO emissions.

On a fleet average basis, NH_3 emissions were slightly higher for the aged catalysts compared with the as-received catalysts for each of the test cycles. The effect of catalyst age was not consistent between the different vehicles, as shown in Figure 3, and the catalyst differences for NH_3 emissions were not statistically significant for any of the cycles. In a larger study, however, differences between the aged and as-received catalyst were found to be statistically significant for both the FTP and the US06, with higher NH_3 emission found for the aged catalysts (*32*).

3.2. Real-Time NH₃ Emissions. To better understand the effects of different driving modes and cycles on NH_3 emissions, it is useful to examine the real-time emissions data. The second-by-second NH_3 emissions for a ULEV vehicle with the OE catalyst are shown in Figure 4 for the FTP and NYCC and in Figure 5 for the US06 and MEC01v7 cycle. Similar trends were also found for each of the remaining vehicles, with the exception of SU1, which showed little increase in NH_3 emissions even under aggressive driving conditions. The real-time emissions data show that NH_3 emissions are primarily generated during acceleration events, with higher NH_3 being generated for more aggressive accelerations. Beyond acceleration events, the NH_3 emissions remain relatively low and for the most part are independent of the driving trace. The observation of higher NH_3 emissions during acceleration can be attributed to higher VSP events and conditions where rich equivalence ratios (λ) are found,
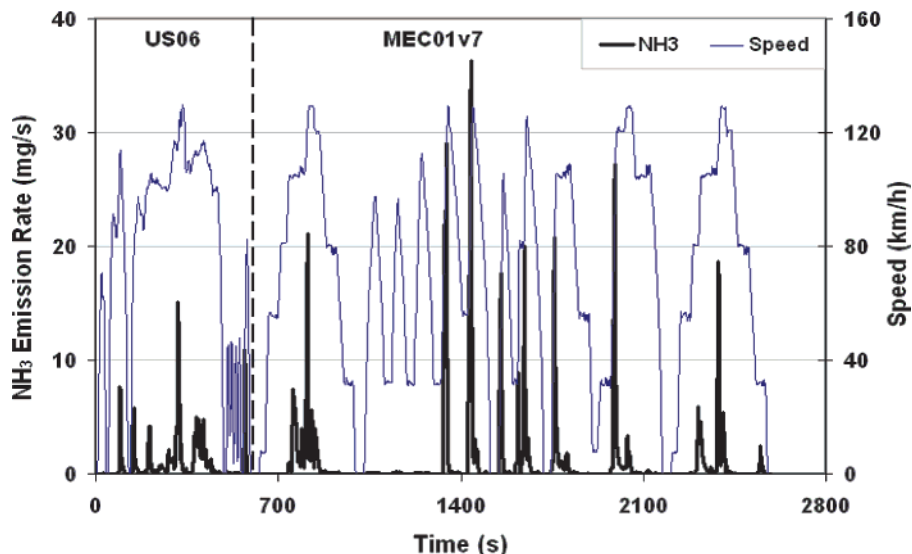
FIGURE 5. Second-by-second NH$_3$ emissions for the US06/MEC01v7 (vehicle U2, OE Cat.).

as discussed below. Some NH$_3$ emissions were also observed during the start period, as discussed below.

The contribution of the acceleration periods was compared with those of other types of operation. For an aggressive cycle, such as MEC01v7, NH$_3$ emissions generated during accelerations represented greater than 85% of the total NH$_3$ emissions for the cycle. Decelerations contributed less than 10%, and cruise conditions contributed 1~5% of the total NH$_3$ emissions for the MEC01v7. Similar trends were also found for the US06 cycle with accelerations, decelerations, and cruise conditions representing approximately 75%, 20%, and 5%, respectively, of the total cycle NH$_3$ emissions. For the lower-speed cycles (FTP75, hot running 505, and NYCC), the acceleration peaks are not as strong and represent only 50% of the total combined cycle NH$_3$ emissions. Deceleration and cruise conditions represent 40% and 10%, respectively, of the total combined cycle NH$_3$ emissions. These results show the importance of vehicle operating condition on NH$_3$ emissions.

3.3. NH$_3$ Emissions During FTP Cold/Hot Start. To better understand the contribution of NH$_3$ formed during the period immediately following vehicle start-up, comparisons were made between the emissions from the hot running 505 cycle and those from the cold start bag 1 (cold start) and hot start bag 3 (hot start) of the FTP, respectively. Since the driving cycles are identical, the primary difference between the cycles is the start condition. The true cold start and hot start emissions can thus be determined by subtracting the hot running 505 emissions from those of bag 1 and bag 3 of the FTP. For most of the test vehicles, higher NH$_3$ emissions were found during the cold-start period. This is illustrated in Figure 4 which shows that in addition to the NH$_3$ emissions typically formed during the normal driving cycle, there is a tendency for some vehicles to form higher NH$_3$ emissions immediately after the light-off of the catalyst. This trend is shown in Table 1 for the remaining vehicles. A similar trend was not found for the hot start emissions, however.

It should be noted that Baum et al. examined NH$_3$ emissions for vehicles running hot compared to running cold (5). Overall, the results were mixed with some vehicles showing higher emissions when running cold and some vehicles showing higher emissions with the vehicle running hot. It was suggested that the vehicles with higher NH$_3$ emissions during the cold running conditions probably had already reached an equilibrium catalyst temperature. Since Baum et al. did not provide a full characterization of NH$_3$ emissions as a function of time during the cold start, these

TABLE 1. Comparison of Start NH$_3$ Emissions[a]

vehicle	catalyst	hot running 505	FTP Bag1 cold start	FTP Bag3 hot start	CS-505	HS-505
SU1	OE	N/A	0.003	0.000	N/A	N/A
	aged	0.003	0.004	0.002	0.001	−0.001
SU2	OE	N/A	0.006	0.001	N/A	N/A
	aged	0.001	0.004	0.000	0.003	−0.001
U1	OE	0.002	0.012	0.007	0.010	0.006
	aged	0.001	0.009	0.002	0.007	0.001
U2	OE	0.001	0.021	0.001	0.019	−0.001
	aged	0.001	0.050	0.000	0.050	−0.001
L1	OE	0.013	0.044	0.024	0.031	0.012
	aged	0.009	0.054	0.002	0.045	−0.007
L2	OE	0.002	0.001	0.000	−0.001	−0.002
	aged	0.001	0.002	0.001	0.001	−0.001
L3	OE	0.001	0.001	0.001	−0.001	−0.001
	aged	0.001	0.005	0.001	0.004	−0.001
L4	OE	0.018	0.021	0.009	0.003	−0.008
	aged	0.050	0.062	0.042	0.012	−0.007

[a] Unit: g/km.

results are not directly comparable to those in the present study.

3.4. NH$_3$ Emissions and Vehicle Specific Power. To further investigate the impacts of specific driving events on NH$_3$ emissions, the relationship between NH$_3$ emissions and VSP was examined. VSP is defined here as the instantaneous power per unit mass of the vehicle. The equation utilized for VSP is similar to that reported by Jimenez-Palacios (1). In the present case, the actual dynamometer road load coefficients are available, so these were utilized in place of similar terms in the equation used by Jimenez-Palacios (1). The VSP equation used in the present study is as follows

$$\text{VSP (kW/metric ton} = m^2/s^3) =$$
$$v[a\cdot(1 + \epsilon_i) + g\cdot\text{grade} + 9.80665 \cdot(A+B\cdot v+C\cdot v^2)/M]$$

where v = velocity (m/s), a = acceleration (m/s^2), ϵ_i = "mass factor", which is the equivalent translational mass of the rotating components (wheels, gears, shafts, etc.) of the powertrain [We utilize a factor of 0.1 for ϵ_i similar to that used by Jimenez-Palacios (1).], g = acceleration of gravity (m/s^2), grade = vertical rise/horizontal distance (zero in our case), 9.80665 = 1 kg/N, A (kg), B (kg/(km/h)), and C (kg/
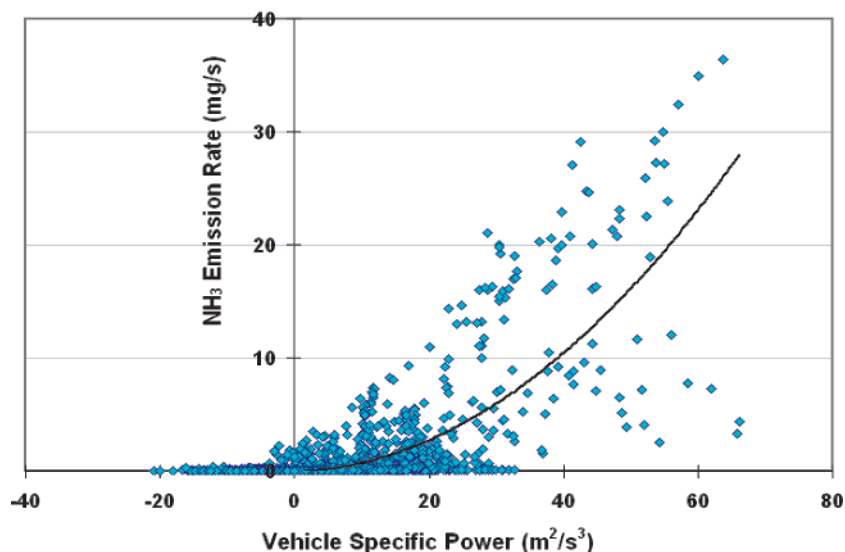
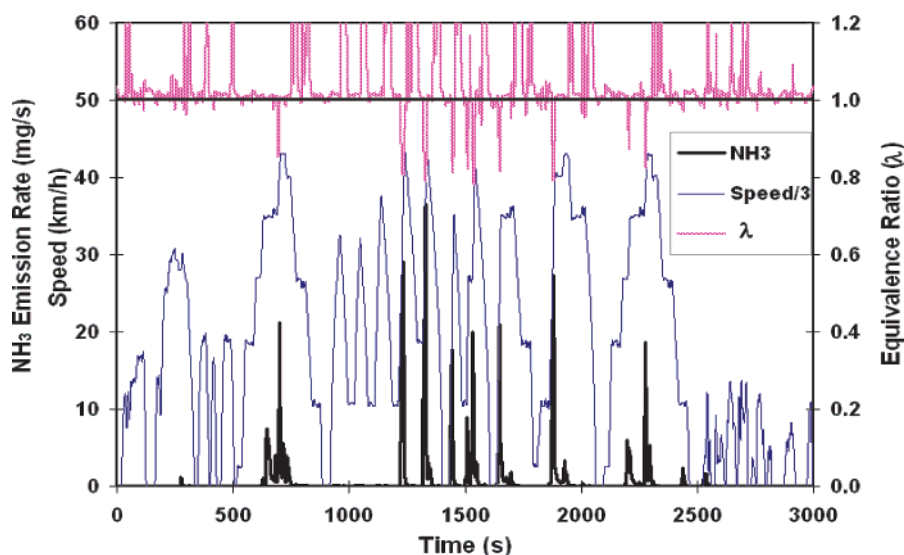FIGURE 6. NH₃ emissions vs vehicle specific power (VSP) (vehicle U2, OE Cat.).

FIGURE 7. Real-time comparison of NH₃ emissions vs equivalence ratio (λ) (vehicle U2, OE Cat.).

$(km/h)^2$) = dynamometer road load coefficients, v = velocity (km/h), and M = vehicle test weight (kg).

A plot of NH₃ emissions against VSP is provided in Figure 6 for the same vehicle shown in Figures 4 and 5. Overall, the NH₃ emissions indicate that VSP is an important factor that should be considered in the modeling of NH₃ emissions. The results show that positive power episodes represent nearly all of the NH₃ emissions for this test. Plots of NH₃ emissions vs VSP for other test vehicles showed very similar trends. The small number of points in the lower right corner of Figure 6, indicating low NH₃ emissions for higher VSP events, can primarily be attributed to peaks where there were slight shifts in the time alignment between the NH₃ peak and the peak in VSP rather than outright anomalies. These points can generally be attributed to only one or two peaks within a typical cycle.

3.5. NH₃ Emissions and Air/Fuel Ratio. The relationship between A/F ratio and NH₃ emissions was also investigated. Specifically, under high VSP conditions, many vehicles are designed to operate under rich A/F ratios to achieve performance objectives. Figure 7 shows a real-time comparison between NH₃ emissions and instantaneous equivalence ratio. These results indicate there is a correlation between A/F ratio and NH₃ emissions, with the highest NH₃

emissions generally found for sharply rich excursions in the equivalence ratio. Although higher NH₃ emissions are found for very rich equivalence ratios, the relationship between NH₃ emissions and equivalence ratio is weaker closer to stoichiometric conditions. Specifically, moderate NH₃ emissions can be found under slightly lean conditions, whereas no NH₃ emissions are found under some slightly rich operating conditions. The observation of generally low NH₃ emissions under lean conditions can probably be attributed to the oxidizing environment on the catalyst surface. These results are consistent with some previous studies, which have shown a strong linear relationship between NH₃ emissions and enrichment (13, 21). In other studies, however, high NH₃ emissions were found even when A/F ratios were not rich (6).

4. Discussion

The major results of this study show that a number of factors can contribute to the formation of NH₃ in vehicle exhaust. NH₃ emissions vary considerably and depend on the vehicle with its associated emission control technology and driving cycle. NH₃ emissions increased for all vehicles on aggressive driving cycles. Real-time emissions data show that NH₃ emissions are primarily generated during acceleration events.

More specifically, higher NH_3 emissions were found under high VSP events with rich A/F ratios. For some vehicles, NH_3 emissions are also formed in the period immediately after catalyst light-off.

While this study provides insight into the effects of various operational parameters and NH_3 emissions in vehicle exhaust, further study is needed to provide a better framework for understanding and modeling the complex relationships and chemistry associated with NH_3 emissions from vehicles. The fleet utilized in this study, for example, is primarily representative of late model technologies that contribute a growing but small portion of the total vehicle population. For current purposes, it is also important to examine a wider range of vehicles to better understand how these relationships change for older technologies and high emitters. It may also be important to better understand the relative impact of catalyst composition and engine-out emissions on NH_3 emissions. Some more detailed catalyst experiments may also be worthwhile, to further investigate any relationships found.

Additional research on developing modal emission models for NH_3 is planned in conjunction with this study. First, the modal NH_3 emissions data will be used to calculate NH_3 emission rates using a VSP binning methodology, as proposed for EPA's MOVES modeling framework (2). Additionally, parameter sets for the College of Engineering, Center for Environmental Research and Technology (CE-CERT)'s Comprehensive Modal Emission Model (CMEM) will be estimated for each vehicle as well as for a composite vehicle (30). While the number of vehicles that will be used in the development of the NH_3 module will be limited, it will provide information for the assessment of the data needs for including NH_3 in a broader context of emissions models.

Acknowledgments

Supporting Information Available

Description of test vehicles (Table 1), properties of the test fuel (Table 2), summary of emissions (Table 3), and summary of correlation coefficients of equivalence ratio vs tailpipe-out NH_3 emissions (Table 4). This material is available free of charge via the Internet at http://pubs.acs.org.

Literature Cited

(1) Jimenez-Palacios, J. L. Ph.D. Dissertation, Massachusetts Institute of Technology, 1999.
(2) Koupal, J.; Michaels, H.; Cumberworth, M.; Bailey, C.; Brzezinski, D. *EPA's Plan for MOVES: A Comprehensive Mobile Source Emissions Model;* Proceedings of the 12th CRC On-Road Vehicle Emissions Workshop, San Diego, CA, April 15−17, 2002.
(3) Frey, H. C.; Unal, A. *Recommended Strategy for On-Board Emission Data Analysis and Collection for the New Generation Model;* Proceedings of the 12th CRC On-Road Vehicle Emissions Workshop, San Diego, CA, April 15−17, 2002.
(4) Baronick, J.; Heller, B.; Lach, G.; Ramacher, B. *SAE Techn. Pap. Ser.* **2000**, No. 2000-01-0857.
(5) Baum, M. M.; Kiyomiya, E. S.; Kumar, S.; Lappas, A. M.; Lord, H. C. III *Environ. Sci. Technol.* **2000**, *34*, 2851−2858.
(6) Baum, M. M.; Kiyomiya, E. S.; Kumar, S.; Lappas, A. M.; Kapinus, V. A.; Lord, H. C. III *Environ. Sci. Technol.* **2001**, *35*, 3735−3741.
(7) Durbin, T. D.; Wilson, R. D.; Norbeck, J. M.; Miller, J. W.; Huai, T.; Rhee, S. *Atmos. Environ.* **2002**, *36*, 1475−1482.
(8) Fraser, M. P.; Cass, G. R. *Environ. Sci. Technol.* **1998**, *32*, 3535−3539.
(9) Gertler, A. W.; Sagebiel, J. C.; Cahill, T. A. *Measurements of Ammonia Emissions from Vehicles in a Highway Tunnel;* Proceedings of the 11th CRC On-road Vehicle Emissions Workshop, San Diego, CA, March 26−28, 2001.
(10) Graham, L. *Gaseous and Particulate Matter Emissions from In−Use Light-duty Gasoline Motor Vehicles;* Report #99-67; Environment Canada, Environmental Technology Center, Emissions Research and Measurement Division: Canada, 1999.
(11) Kean, A. J.; Harley, R. A.; Littlejohn, D.; Kendall, G. R. *Environ. Sci. Technol.* **2000**, *32*, 3535−3539.
(12) Moeckli, M. A.; Fierz, M.; Sigrist, M. W. *Environ. Sci. Technol.* **1996**, *30*, 2864−2867.
(13) Shores, R. C.; Walker, J.; Kimbrough, S.; McCulloch, R. B.; Rodgers, M. O.; Pearson, J. R. *Measurements of Ammonia Emissions from EPA's Instrumented Vehicles.* Proceedings of the 10th CRC On-Road Vehicle Emissions Workshop, San Diego, CA, March 27−29, 2000.
(14) *Unregulated Motor Vehicle Exhaust Gas Components;* Internal Publication of Volkswagen AG Research and Development, F.R., Germany, 1989.
(15) Chitjian, M.; Koizumi, J.; Botsford, C. W.; Mansell, G.; Winegar, E. *Final 1997 Gridded Ammonia Emission Inventory Update for the South Coast Air Basin;* Final Report to the South Coast Air Quality Management District under contract 99025; August 2000.
(16) Harvey, C. A.; Garbe, R. J.; Baines, T. M.; Somers, J. H.; Hellman, K. H.; Carey, P. M. *SAE Techn. Pap. Ser.* **1983**, No. 830987.
(17) Smith, L. R.; Carey, P. M. *SAE Techn. Pap. Ser.* **1982**, No. 820783.
(18) Urban, C. M.; Garbe, R. J. *SAE Techn. Pap. Ser.* **1979**, No. 790696.
(19) Urban, C. M.; Garbe, R. J. *SAE Techn. Pap. Ser.* **1980**, No. 800511.
(20) Bradow, R. L.; Stump, F. D. *SAE Techn. Pap. Ser.* **1977**, No. 770369.
(21) Cadle, S. H.; Nebel, G. J.; Williams, R. L. *SAE Techn. Pap. Ser.* **1979**, No. 790694.
(22) Cadle, S. H.; Mulawa, P. A. *Environ. Sci. Technol.* **1980**, *14*, 718−723.
(23) Shelef, M.; Gandhi, H. S. *Ind., Eng. Chem., Prod. Res., Dev.* **1972**, *11*, 2.
(24) Shelef, M.; Gandhi, H. S. *Ind., Eng. Chem., Prod. Res., Dev.* **1972**, *11*, 393.
(25) Gandhi, H. S.; Piken, A. G.; Stepien, H. K.; Shelef, M.; Delosh, R. G.; Heyde, M. E. *SAE Techn. Pap. Ser.* **1977**, No. 770196.
(26) Gandhi, H. S.; Shelef, M. *Ind. Eng. Chem., Prod. Res. Dev.* **1974**, *13*, 80.
(27) Gandhi, H. S.; Shelef, M. *Appl. Catal.* **1991**, *77*, 175−186.
(28) Hirano, H.; Yamada, T.; Tanaka, K. I.; Siera, J.; Cobden, P.; Nieuwenhuys, B. E. *Surf. Sci.* **1992**, *262*, 97−112.
(29) Nieuwenhuys, B. E. *Adv. Catal.* **2000**, *44*, 259−328.
(30) Barth, M.; An, F.; Younglove, T.; Scora, G.; Levine, C.; Ross, M.; Wenzel, T. *Development of a Comprehensive Modal Emissions Mode;* Final Report by the University of California's Bourns College of Engineering-Center for Environmental Research and Technology, Riverside, CA for the National Cooperative Highway Research Program under contract NCHRP 25-11; 2000.
(31) Sims, G. S.; Johri, S. *SAE Techn. Pap. Ser.* **1988**, No. 881589.
(32) Durbin, T. D.; Miller, J. W.; Pisano, J. T.; Younglove, T.; Sauer, C.; Rhee, S. H.; Huai, T.; MacKay, G. I. *The Effect of Sulfur and NH₃ and other Regulated Emissions from 2000 to 2001 Model Year Vehicles;* Final Report for the Coordinating Research Council Project E-60, by the University of California's Bourns College of Engineering-Center for Environmental Research and Technology; Riverside, CA, May 2003.
(33) Muecke, R.; Werle, P.; Slemr, F.; Pretl, W. *Comparison of time and frequency multiplexing techniques in multicomponent FM spectroscopy.* In *Measurement of Atmospheric Gase;* Schiff, H. I., Ed.; 1991; SPIE 1433, pp 136−142.
(34) Kitagawa, H.; Mibe, T.; Okamatsu, K.; Yasui, Y. *SAE Techn. Pap. Ser.* **2000**, No. 2000-01-0887.